RAA 2020 Vol. **20** No. **6**, 88(8pp) doi: 10.1088/1674–4527/20/6/88

http://www.raa-journal.org *http://iopscience.iop.org/raa*

Research in Astronomy and Astrophysics

Site-testing at Muztagh-ata site III: temperature inversion in surface-layer atmosphere

Jing Xu[1,2], Ali Esamdin[1,2], Guo-Jie Feng[1,2], Guang-Xin Pu[1], Yi Hu[3], Ke-Liang Hu[3], Xu Yang[3], Jin-Xin Hao[3], Yan-Jie Xue[3], Xu Zhou[3], Shu-Guo Ma[1], Abudusaimaitijiang Yisikandee[1], Le-Tian Wang[1], Xuan Zhang[1], Chun-Hai Bai[1], Peng Wei[1], Liang Ming[1], Lu Ma[1], Jin-Zhong Liu[1] and Yun-Ying Jiang[3]

[1] Xinjiang Astronomical Observatory, Chinese Academy of Sciences, Urumqi 830011, China; *xujing@xao.ac.cn, aliyi@xao.ac.cn*

[2] University of Chinese Academy of Sciences, Beijing 100049, China

[3] National Astronomical Observatories, Chinese Academy of Sciences, Beijing 100101, China

Received 2020 April 21; accepted 2020 May 18

Abstract In this article, we present detailed seasonal, monthly and daily statistics of temperature difference in the surface layer at the Muztagh-ata site based on the temperature measurements at two heights of 2 m and 6 m. We find that temperature inversion occurs frequently at our site during nighttime, especially during the cold season. Strong temperature inversion always represents stable atmospheric turbulence, which is crucial for an optical observatory. By analyzing the behavior of temperature inversion and its correlation with wind and cloud amount, one conclusion can be made that radiation inversion is the main reason for the existence of temperature inversion in the surface-layer at the Muztagh-ata site.

Key words: site-testing — atmospheric turbulence — temperature inversion

1 INTRODUCTION

Located at an altitude of 4520 m on the Pamir Plateau in western China, the Muztagh-ata site has undergone an intense site-testing campaign for more than three years (Feng et al. 2020), with the other two candidate sites being Ali (Liu et al. 2020) and Daocheng (Song et al. 2020). Already showing excellent optical observation conditions, such as ground meteorology (Xu et al. 2020a), seeing conditions (Xu et al. 2020b) and amount of clouds (Cao et al. 2020a,b), the Muztagh-ata site is predicted to hopefully host China's future Large Optical/infrared Telescope (LOT) project.

As important characteristic for optical observatories, temperature and wind speed gradients result in the formation of optical turbulence, while the spatial and temporal stability of these quantities in turn determine the performance of Adaptive Optics (AO) systems (Aristidi et al. 2005). When it comes to the temperature and wind speed profiles through the atmosphere, weather balloons (Aristidi et al. 2005) and the SLODAR technique (Sivo et al. 2018) are usually employed for acquiring temperature and wind speed values higher than 100 m. Near-surface wind and temperature structures usually play a pivotal role in determining the momentum and energy exchange between the Earth's surface and the atmosphere (Zhou et al. 2009). Aristidi et al. (2009) found that the median value of the boundary layer height at Antarctic Dome C is 33 m. Bonner et al. (2010) reported a median boundary layer height of 13.9 m for Antarctic Dome A. Stable atmospheric activity in the near-surface layer is crucial for atmospheric seeing at these plateau sites. The thickness and intensity of the turbulent surface layer usually increase with wind speed (Ehgamberdiev et al. 2000; Travouillon et al. 2003). But beyond wind, the phenomenon of temperature inversion also comes from atmospheric structure. With steady wind flow, temperature inversion demonstrates the stability of atmospheric structure near the ground. Hu et al. (2014) and Hu et al. (2019) found strong and lasting temperature inversion frequently occurs at Antarctic Dome A. Such temperature inversion existed at all heights above the ground most of the time in 2015 and 2016. We also found that the seeing behavior correlates with near-surface temperature inversion at the Muztagh-ata site (Xu et al. 2020b). For exploring behavior and the main reasons for temperature inversion, we have monitored the temperature gradient in the past two years. In this paper, we present the results from analyzing continuous temperature gradi-

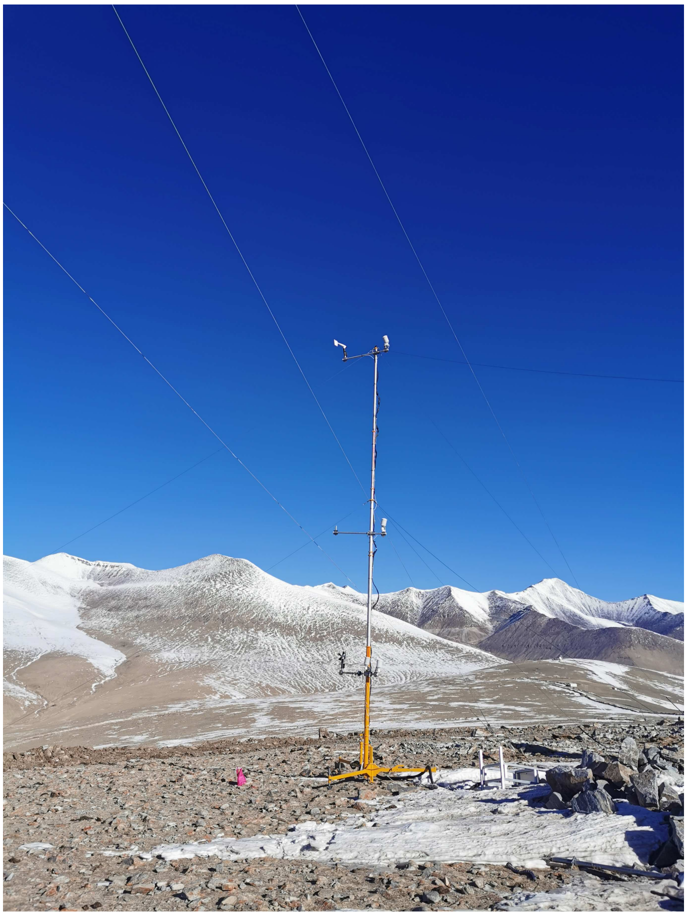

Fig. 1 KLAWS-2G installed at the Muztagh-ata site.

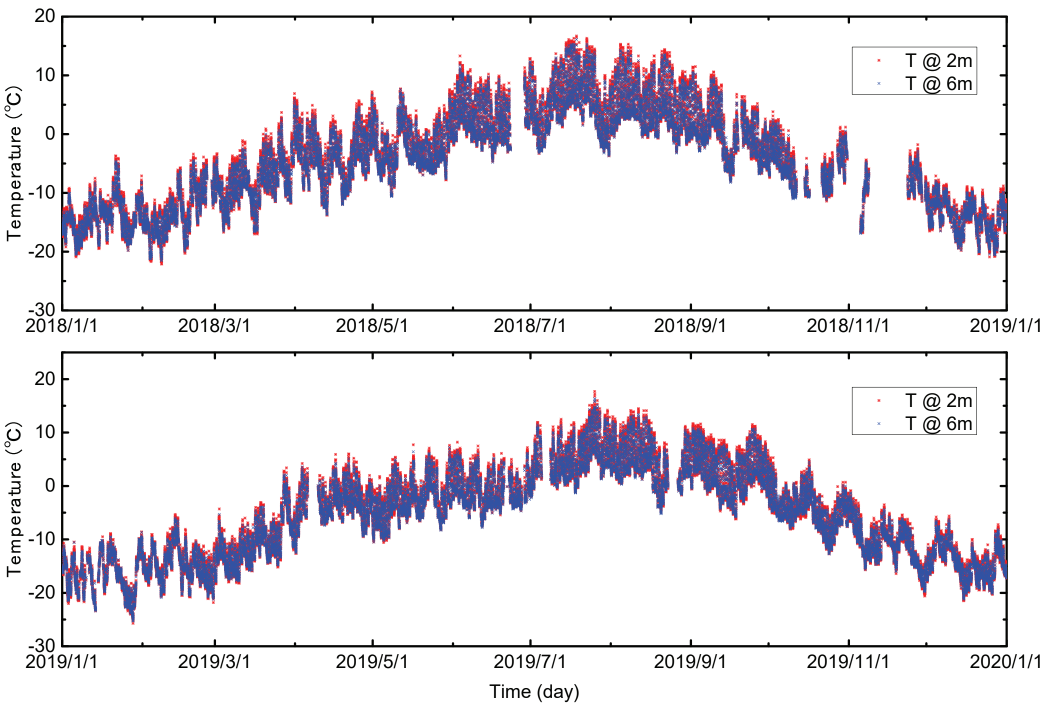

Fig. 2 Temperature at 2 m and 6 m with time during 2018 (*top*) and 2019 (*bottom*).

ent data for these two years. The monitoring observation is briefly described in Section 2. Detailed statistical analysis of temperature inversion is shown in Section 3. We give a simple analysis of conditions formed from inversion in Section 4. Finally, a discussion and summary are presented in Section 5.

2 MONITORING OBSERVATION

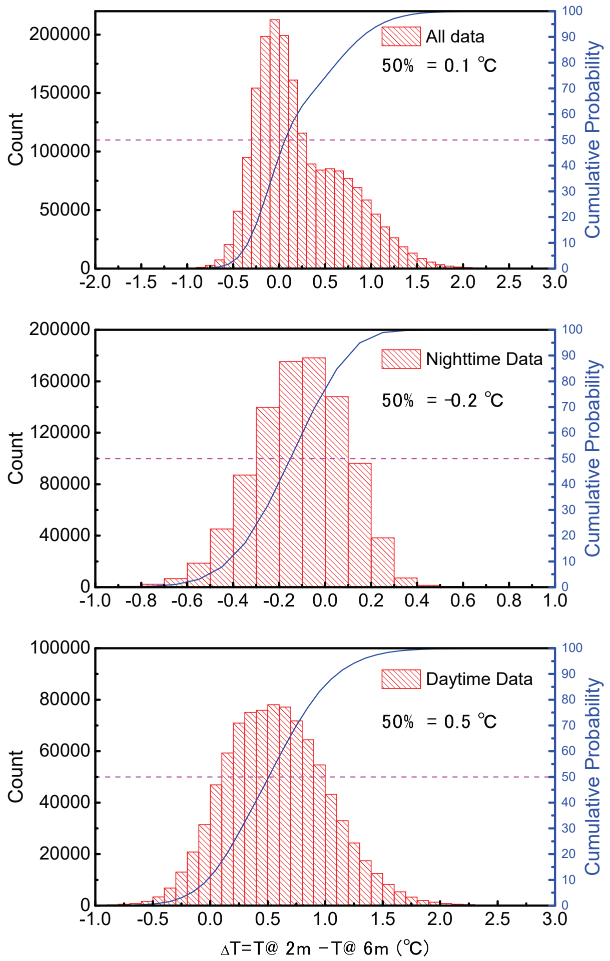

Fig. 3 Distribution and cumulative statistics of $\triangle T$ during the whole measurement, nighttime and daytime periods from *top* to *bottom* respectively.

An automated weather station named second generation Kunlun Automated Weather Station (KLAWS-2G)[1] was installed at the Muztagh-ata site and started to record data from spring of 2017. Detailed information about KLAWS-2G and calibration can be referenced in Hu et al. (2019). We were planning to get temperature and wind speed gradient data for four heights (at 2, 6, 10 and 15 m). But unfortunately, not long after installation, the station

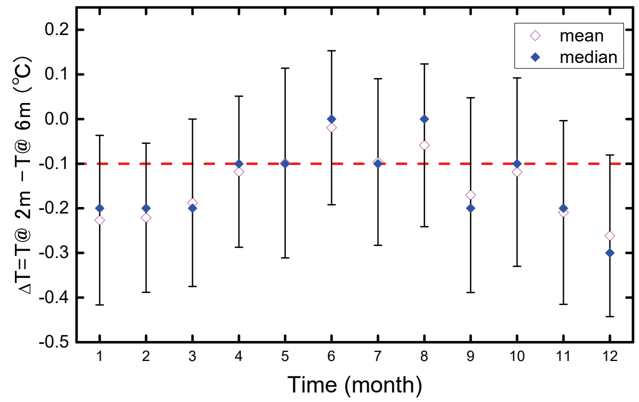

Fig. 4 Monthly statistics of $\triangle T$ during nighttime.

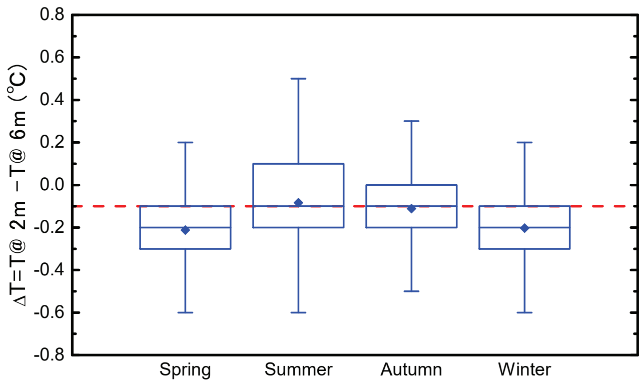

Fig. 5 Seasonal nighttime statistics of $\triangle T$. Each box represents values in the range of 25% to 75% and vertical lines mark the values 1% to 99%. The *diamonds* and *horizontal lines* inside the boxes correspond to mean and median values respectively. The *red dashed line* signifies $-0.1°$ C of $\triangle T$.

was blown down by wind and several sensors were damaged. From the beginning of 2018 to the end of 2019, there were temperature sensors at 6 m and 2 m collecting data regularly. The monitoring project was finished at the beginning of 2020 when the site begin construction for new telescopes. Figure 1 depicts the KLAWS-2G installed at the Muztagh-ata site.

According to the parameters given by the manufacturer, uncertainty in all temperature measurements of the Young 41342 temperature sensor used on KLAWS-2G is $0.32°$ C. However, it should be more accurate to less than $0.1°$ C as the test results in Hu et al. (2014) reported. So, the accuracy of the Young 41342 sensor satisfies the temperature inversion measurement.

Figure 1 plots temperature at 2 m and 6 m with time during 2018 and 2019 respectively. The sampling period of KLAWS-2G is 30 s. From 2018 January 1 to 2019 December 31, there were 674 days in total that have gradient data, accounting for 92.3% of the two-year measurement period. We can see from Figure 1 that there is an obvious data gap in the winter of 2018, which was caused by

[1] `http://aag.bao.ac.cn/xjtest/index.php`

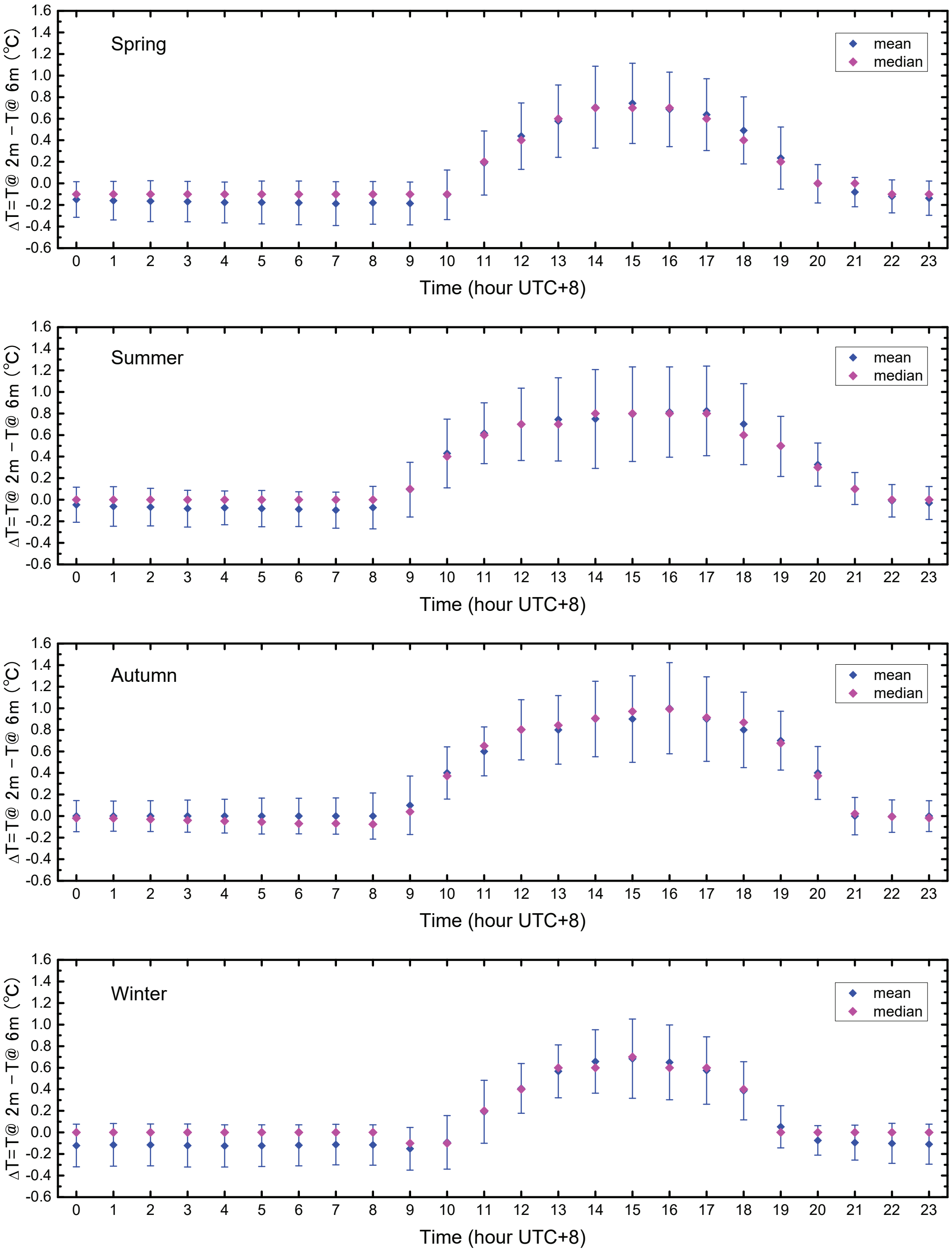

Fig. 6 Mean and median values of hourly $\triangle T$ for spring, summer, autumn and winter.

failure of the computer. The other missing data are mainly caused by power failure.

3 STATISTICAL RESULTS

The phenomenon of temperature inversion means that there is a positive correlation between air temperature and elevation. To investigate the frequency of temperature inversion at the Muztagh-ata site, we display distributions and cumulative curves of temperature differences between 2 m and 6 m during the whole period, nighttime and daytime (we define the time from the beginning of astronomical morning twilight to the end of astronomical evening twilight as daytime, and the rest of this day as nighttime) separately in Figure 3. Here we define $\triangle T = T(2\,\mathrm{m}) - T(6\,\mathrm{m})$ to represent the strength of inversion. The median values of $\triangle T$ are 0.1° C, -0.2° C and 0.5° C during the whole time, nighttime and daytime respectively. Considering the accuracy of the sensor, we believe that when the value

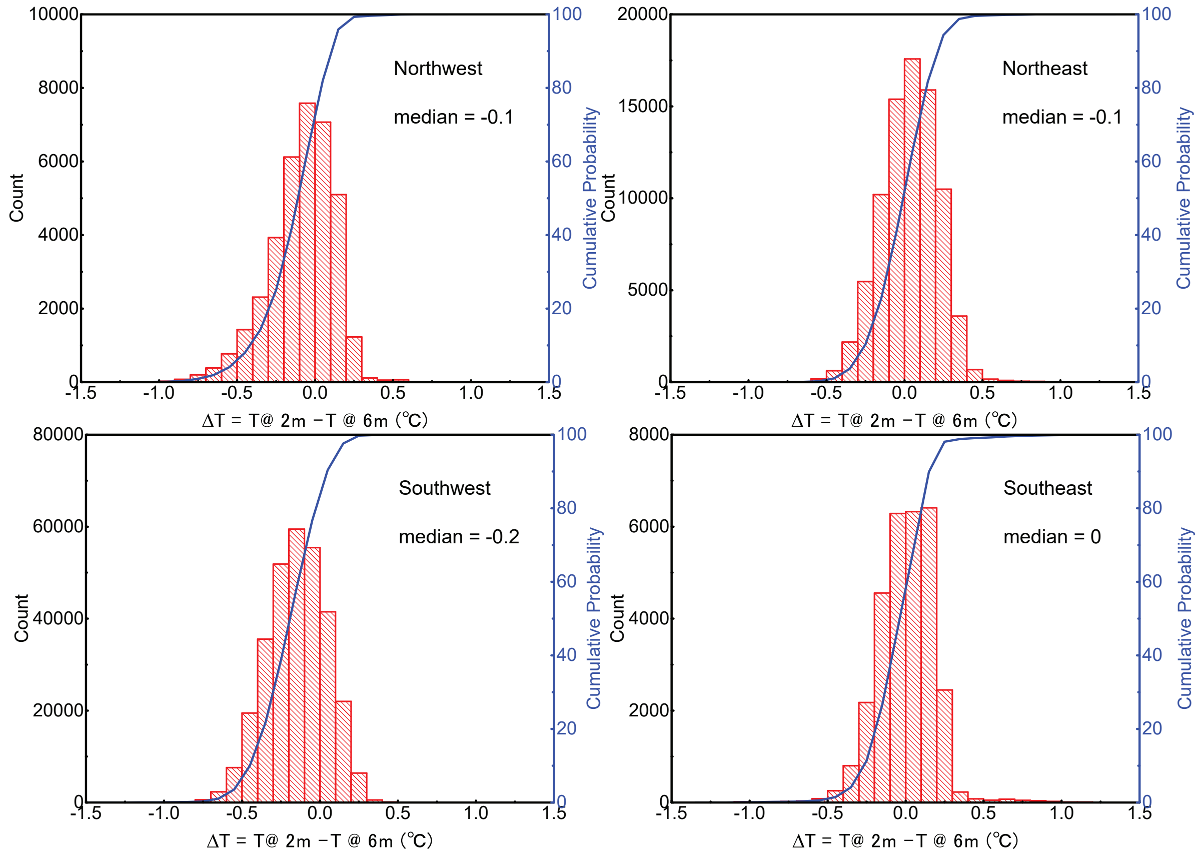

Fig. 7 Distribution and cumulative distribution functions of $\triangle T$ in four ranges of wind direction.

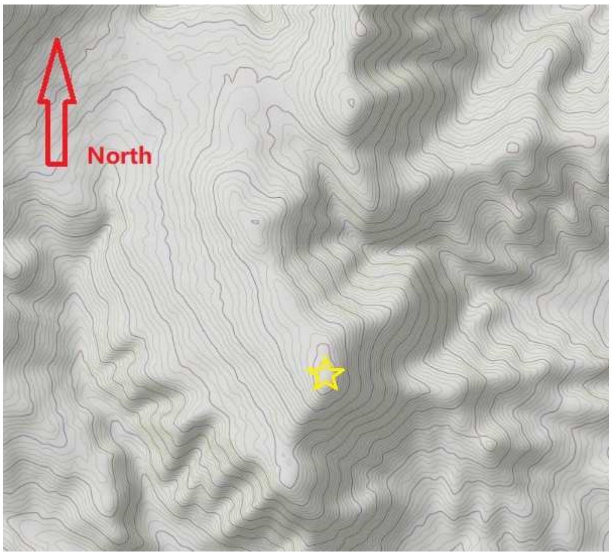

Fig. 8 Contour map of the region surrounding the Muztagh-ata site. The *yellow pentagram* marks the location of our monitoring equipments at present.

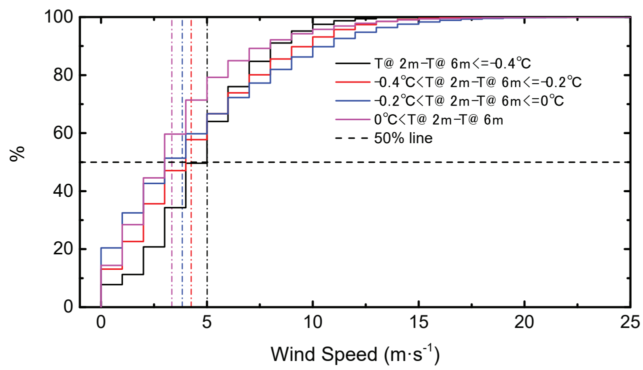

Fig. 9 Cumulative distribution functions of wind speed in four ranges of $\triangle T$: smaller than -0.4° C (*black*), $-0.4 \sim -0.2^{\circ}$ C (*red*), $-0.2 \sim 0^{\circ}$ C (*blue*) and higher than 0° C (*pink*).

of $\triangle T$ is less than -0.1° C, the inversion definitely occurs. During nighttime, 54.6% of the time, $\triangle T$ is less than 0° C, which indicates that the inversion exists more than half of the nighttime at the Muztagh-ata site. We have found that temperature inversion occurs more than 70% of time around the middle of the night. (Xu et al. 2020b).

Monthly variation of $\triangle T$ during nighttime is shown in Figure 4, in which pink diamonds represent mean values for each month while blue ones signify medians. The minimum monthly mean value is -0.26° C in December and the maximum is -0.02° C in June. Overall, temperature inversion is stronger in the cold season than in the warm season. Seasonal nighttime statistics are featured in

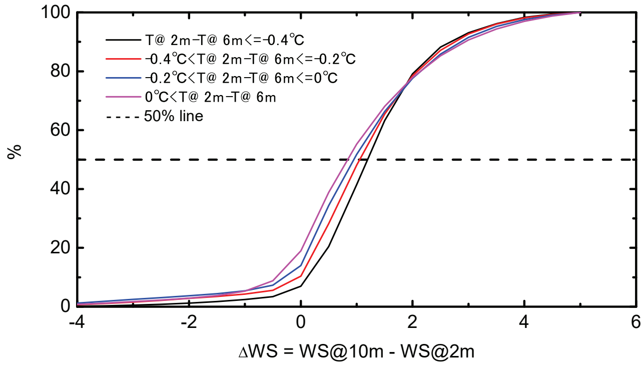

Fig. 10 Cumulative distribution functions of $\triangle WS$ in four ranges of $\triangle T$: smaller than $-0.4°$ C (*black*), $-0.4 \sim -0.2°$ C (*red*), $-0.2 \sim 0°$ C (*blue*) and higher than $0°$ C (*pink*).

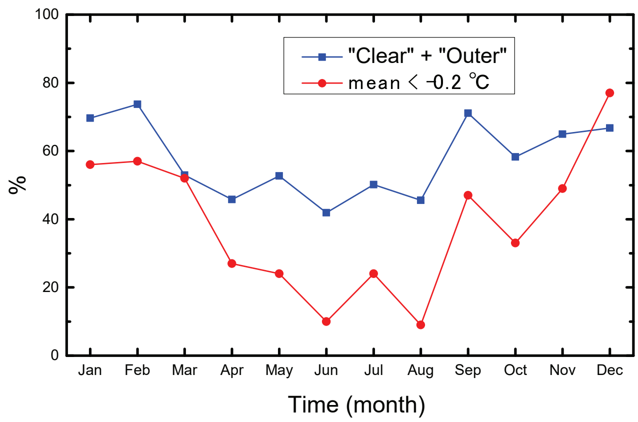

Fig. 11 Monthly observable time (*blue*) and proportion of days with mean temperature difference during nighttime less than $-0.2°$ C (*red*).

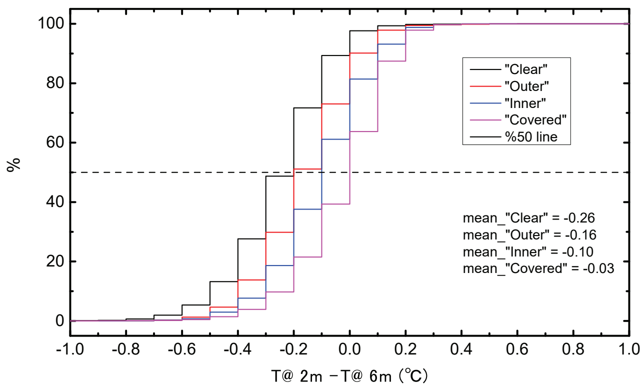

Fig. 12 Cumulative distribution functions of temperature difference in four cases of cloud amount: “clear” (*black*), “outer” (*red*), “inner” (*blue*) and “covered” (*pink*).

Figure 5, in which each box represents the values in the range of 25% to 75% and vertical lines signify the values 1% to 99%. The diamonds and horizontal lines inside the boxes correspond to mean and median values respectively. The minimum seasonal mean value is $-0.21°$ C in spring while the maximum is $-0.08°$ C in summer. The red dashed line indicates $\triangle T$ of $-0.1°$C. In spring and winter, 75% of the time during night $\triangle T$ is less than $-0.1°$ C, while in summer and autumn the rate is about 50%.

The 24 hour variation of $\triangle T$ is displayed in Figure 6 where hourly medians and means are computed after merging different days. We plot the hourly results for each season integrated over the acquisition period (spring, summer, autumn and winter from top to bottom respectively). It can be clearly seen that the surface-layer temperature inversion usually occurs after sunset and reaches its lowest value before sunrise.

4 CORRELATION WITH AMOUNT OF WIND AND CLOUDS

To explore the conditions for existence of the surface layer at the Muztagh-ata site, we show the relationship between $\triangle T$ and nighttime surface wind in Figure 7 and Figure 9. The surface wind speed and direction values were acquired from the anemometer set at 2 m on KLAWS-2G. The wind speed and direction values were collected synchronously with temperature sensors.

In Figure 7, we present the distribution and cumulative distribution functions of $\triangle T$ in four wind direction ranges during nighttime. The median values of the four ranges are $-0.1°$ C (northwest), $-0.1°$ C (northeast), $-0.2°$ C (southwest) and $0°$ C (southeast) respectively. When wind comes from the southwest, the temperature inversion gets stronger than in other directions. Figure 8 depicts the topographical conditions surrounding the Muztagh-ata site. The southwest of the mountain has a gentle slope and the terrain in this direction is much simpler than others. Wind coming from the southwest will not cause strong turbulence in the air above our site. Fortunately, the prevailing wind direction is southwest at our site (Xu et al. 2020a).

The four cumulative distribution functions of wind speed in Figure 9 represent four ranges of $\triangle T$: smaller than $-0.4°$ C (black), $-0.4 \sim -0.2°$ C (red), $-0.2 \sim 0°$ C (blue) and higher than $0°$ C (pink). The median wind speeds of the four $\triangle T$ ranges are 5.02 m s^{-1}, 4.26 m s^{-1}, 3.84 m s^{-1} and 3.34 m s^{-1}. In the condition of certain surface wind velocities, the inversion gets stronger.

During most of 2018, two vanes worked well set at 10 m and 2 m respectively. To illustrate the relationship between vertical wind shear and inversion, we define $\triangle WS = WS(10\,\mathrm{m}) - WS(2\,\mathrm{m})$ and plot Figure 10. The median values of $\triangle WS$ in the four ranges of $\triangle T$ are 1.18 m s^{-1}, 1.04 m s^{-1}, 0.92 m s^{-1} and 0.82 m s^{-1}. From this plot, we can see that the increase in vertical wind speed difference usually occurs when temperature inversion gets stronger.

From Figure 4 and Figure 5, a clear seasonal dependence of surface-layer inversion can be seen. In summer and autumn, more precipitation occurs than in spring and winter at the Muztagh-ata site. In Figure 11, a blue line represents the monthly percentages of observable nighttime (the allsky images classified as "clear" and "outer," relative definition and results can be ascertained in Cao et al. (2020a). The red line signifies the proportion of days with mean temperature difference during nighttime less than -0.2° C for each month. The relationship between inversion and cloud amount is demonstrated in Figure 12. Four cumulative curves in the plot correspond to $\triangle T$ in four cases of cloud amounts: "clear," "outer," "inner" and "covered." The mean temperature difference values are -0.26° C, -0.16° C, -0.1° C and -0.03° C for the four cases respectively, which indicates that surface-layer temperature inversion is stronger with reduction in amount of clouds.

5 DISCUSSION AND SUMMARY

By analyzing the temperature data from KLAWS-2G during 2018 and 2019, we found surface-layer temperature inversion occurs frequently at the Muztagh-ata site. When there is a breeze, strong inversion always represents stable atmospheric turbulence. We have studied the seasonal, monthly and daily trends of temperature inversion in the surface-layer atmosphere and its dependence on amount of wind and clouds. Then we explored the relationship between inversion and some meteorological parameters. We found such features of inversion at Muztagh-ata are as follows:

1. The surface-layer temperature inversion is stronger in cold months than in warm months at the Muztagh-ata site. More stable atmospheric structure near-ground is one reason that the seeing is better in the cold season at our site.

2. Daily trends show that the strongest surface-layer inversion during one night usually occurs toward dawn.

3. The relationship between wind and surface-layer temperature inversion indicates that in the condition of certain surface wind velocity, the inversion becomes stronger with increasing vertical wind shear. When it blows from the southwest, the temperature inversion gets stronger than the wind from other directions.

4. By analyzing cloud amount results, we found that stronger inversion occurs more frequently during clear nights.

We are aware that using only two heights for temperature is not good enough to illustrate the distribution of surface-layer turbulence, but it is useful to acquire some preliminary conclusion on characteristics and origins of surface-layer inversion. The formation of inversion is often the result of several factors such as radiation, advection, turbulence, etc.

Temperature inversion caused by radiation often occurs in the middle and high latitudes, especially in desert areas. This temperature inversion is usually strongest in winter while weakest in summer. After sunset, the temperature of the ground decreases due to radiative cooling, and the temperature of the air in the layer close to the ground decreases faster than air in the upper layer, so temperature inversion occurs. With continuous effective radiation throughout the night, the temperature inversion gets stronger gradually and reaches the peak toward dawn. After sunrise, with the increases of solar radiation, both the temperature of the ground and the air near ground rise quickly, so the temperature inversion disappears. From the seasonal, monthly and hourly statistics, we can find that the behavior of temperature inversion at Muztagh-ata accords with the feature of radiation inversion.

Statistics on the dependence of temperature inversion on wind and amount of clouds demonstrate that strong temperature inversion could well happen during clear nights with a breeze from the southwest at the Muztagh-ata site. A moderate wind cannot cause a strong vertical mixing effect in the atmosphere, which will prevent air near the ground from cooling down. Because the cooling effect can be brought to the upper layer of the atmosphere by moderate wind, it is beneficial to thicken the temperature inversion layer. Clouds can weaken effective radiation from the ground and stop it from cooling down, so temperature inversion often occurs during clear nights. When strong temperature inversion occurs, the difference between wind speed at different heights increases. This is because the temperature inversion blocks momentum transfer between the upper and lower air and results in the difference in wind speed.

In conclusion, radiation inversion is the main cause of temperature inversion at the Muztagh-ata site. The inversion layer is strongest in winter and weakest in summer, especially during clear nights with moderate wind. Topographically, the terrain is more gentle in the southwest of the mountain than other directions and the wind from this direction will not disturb the atmospheric structure at the surface layer. The statistics of temperature inversion for different wind directions demonstrate this. It is dominated by southwest wind all-year round in this area and the wind from other directions has little effect on the turbulence. In the future, we plan to install a temperature and wind speed gradient tower about 30 m high for long-term measurements to explore the more accurate structure of near-ground turbulence at the Muztagh-ata site.

Acknowledgements This work is supported by the National Natural Science Foundation of China (Grant

Nos. 11873081 and 11803076) and the Operation, Maintenance and Upgrading Fund for Astronomical Telescopes and Facility Instruments, budgeted from the Ministry of Finance of China (MOF) and administered by the Chinese Academy of Sciences (CAS).

References

Aristidi, E., Agabi, A., Azouit, M., et al. 2005, EAS Publications Series, 14, 227
Aristidi, E., Agabi, K., Azouit, M., et al. 2005, A&A, 430, 739
Aristidi, E., Fossat, E., Agabi, A., et al. 2009, A&A, 499, 955
Bonner, C. S., Ashley, M. C. B., Cui, X., et al. 2010, PASP, 122, 1122
Cao, Z. H., Liu, L. Y., Zhao, Y. H., et al. 2020, RAA (Research in Astronomy and Astrophysics), 20, 81
Cao, Z. H., Hao, J. X., Feng, L., et al. 2020, RAA (Research in Astronomy and Astrophysics), 20, 82
Ehgamberdiev, S. A., Baijumanov, A. K., Ilyasov, S. P., et al. 2000, A&AS, 145, 293
Feng, L., Hao, J. X., Cao, Z. H., et al. 2020, RAA (Research in Astronomy and Astrophysics), 20, 80
Hu, Y., Shang, Z., Ashley, M. C. B., et al. 2014, PASP, 126, 868
Hu, Y., Hu, K., Shang, Z., et al. 2019, PASP, 131, 015001
Liu, L. Y., Yao, Y. Q., Yin, J., et al. 2020, RAA (Research in Astronomy and Astrophysics), 20, 84
Song, T. F., Liu, Y., Wang, J. X., et al. 2020, RAA (Research in Astronomy and Astrophysics), 20, 85
Sivo, G., Turchi, A., Masciadri, E., et al. 2018, MNRAS, 476, 999
Travouillon, T., Ashley, M. C. B., Burton, M. G., et al. 2003, A&A, 400, 1163
Xu, J., Esamdin, A., Hao, J. X., et al. 2020, RAA (Research in Astronomy and Astrophysics), 20, 86
Xu, J., Esamdin, A., Hao, J. X., et al. 2020, RAA (Research in Astronomy and Astrophysics), 20, 87
Zhou, M., Zhang, Z., Zhong, S., et al. 2009, Journal of Geophysical Research (Atmospheres), 114, D17115